Engineering photosynthetic light capture: impacts on improved solar energy to biomass conversion

Jan H. Mussgnug[1,4], Skye Thomas-Hall[2], Jens Rupprecht[1], Alexander Foo[1], Viktor Klassen[4], Alasdair McDowall[1,3], Peer M. Schenk[2], Olaf Kruse[4] and Ben Hankamer[1,]*

[1]*Institute for Molecular Bioscience, The University of Queensland, Brisbane, Qld 4072, Australia*

[2]*School of Integrative Biology, The University of Queensland, Brisbane, Qld 4072, Australia*

[3]*Centre for Microscopy and Microanalysis, The University of Queensland, Brisbane, Qld 4072, Australia*

[4]*Department of Biology/Algae BioTech Group, University of Bielefeld, 33615 Bielefeld, Germany*

Summary

The main function of the photosynthetic process is to capture solar energy and to store it in the form of chemical 'fuels'. Increasingly, the photosynthetic machinery is being used for the production of biofuels such as bio-ethanol, biodiesel and bio-H_2. Fuel production efficiency is directly dependent on the solar photon capture and conversion efficiency of the system. Green algae (e.g. *Chlamydomonas reinhardtii*) have evolved genetic strategies to assemble large light-harvesting antenna complexes (LHC) to maximize light capture under low-light conditions, with the downside that under high solar irradiance, most of the absorbed photons are wasted as fluorescence and heat to protect against photodamage. This limits the production process efficiency of mass culture. We applied RNAi technology to down-regulate the entire LHC gene family simultaneously to reduce energy losses by fluorescence and heat. The mutant *Stm3LR3* had significantly reduced levels of LHCI and LHCII mRNAs and proteins while chlorophyll and pigment synthesis was functional. The grana were markedly less tightly stacked, consistent with the role of LHCII. *Stm3LR3* also exhibited reduced levels of fluorescence, a higher photosynthetic quantum yield and a reduced sensitivity to photoinhibition, resulting in an increased efficiency of cell cultivation under elevated light conditions. Collectively, these properties offer three advantages in terms of algal bioreactor efficiency under natural high-light levels: (i) reduced fluorescence and LHC-dependent heat losses and thus increased photosynthetic efficiencies under high-light conditions; (ii) improved light penetration properties; and (iii) potentially reduced risk of oxidative photodamage of PSII.

Introduction

Photosynthesis is of fundamental biological importance, as almost all life on Earth depends on it, either directly or indirectly via its products. Light-harvesting proteins fulfil a special role in this process as they form the intersect between the physical world (solar electromagnetic radiation) and living cells. Specifically, they capture solar energy and regulate the flow of the derived excitation energy to the photosynthetic reaction centres, in all photosynthetic organisms. The central role of light-harvesting proteins in solar energy capture also makes them key biotechnological targets in any strategy to genetically optimize the efficiency of the synthesis of bio-products and biofuels such as bio-ethanol, biodiesel, bio-H_2 and biomass to liquid (BTL) (Kruse *et al.*, 2005; Rupprecht *et al.*, 2006; Zwart *et al.*, 2006).

Natural antenna diversity

It is perhaps not surprising that the huge diversity of photosynthetic organisms (e.g. purple bacteria, cyanobacteria, green-sulphur bacteria, green algae, lower and higher plants)

have evolved a wide variety of light-harvesting proteins, specialized for their specific habitats (Grossman *et al.*, 1995). In plants and a variety of microalgae (e.g. green algae), these are called light-harvesting complex (LHC) proteins. They are embedded in the thylakoid membranes of the chloroplast and act as structural scaffolds that hold chlorophylls and carotenoids in defined orientations and optimized molecular environments for light capture. Light-harvesting complexes are divided into distinct LHCI and LHCII protein families, based on their predominant association with photosystem (PS) I or II, respectively.

The LHCI protein family comprises several nuclear encoded isoforms [e.g. 6 *LHCA1-6* isoforms in *Arabidopsis thaliana* (Jansson, 1999) and 9 *LHCA1-9* genes in *Chlamydomonas reinhardtii* (Takahashi *et al.*, 2004)] which exhibit high sequence homology. The LHCI proteins provide PSI with the excitation energy necessary to reduce the electron acceptor ferredoxin.

The LHCII proteins are subdivided into the major and minor proteins. The major proteins are far more abundant and largely form trimers making up the outer light-harvesting antenna system. This funnels excitation energy via the inner antenna to the PSII reaction centre. The inner antenna consists of the minor LHCII proteins that are monomeric (Boekema *et al.*, 1995; Hankamer *et al.*, 1997; Dekker and Boekema, 2005).

The LHCII proteins are encoded by a family of nuclear genes and their number and nomenclature vary from species to species [e.g. 9 *LHCB1-3* isoforms in *Arabidopsis thaliana* (Jansson, 1999; Legen *et al.*, 2001); 9 *LHCBM1-11* isoforms in *C. reinhardtii* (Elrad & Grossman, 2004)]. The LHCII genes and proteins share a high degree of sequence similarity, not only to one another but also with the LHCI proteins. The reasons for the evolution of such a large number of highly related proteins and their individual functions are not known but are thought to reflect the great adaptive flexibility required of the photosynthetic machinery. The expression of each isoform is highly regulated from the level of mRNA transcription to protein degradation (Escoubas *et al.*, 1995; Flachmann and Kühlbrandt, 1995; Lindahl *et al.*, 1995; Durnford *et al.*, 2003; Tokutsu *et al.*, 2004; Mussgnug *et al.*, 2005). Furthermore, the translation of individual LHCII isoforms can be regulated by the translational repressor NAB1 through mRNA sequestration (Mussgnug *et al.*, 2005). Additionally, light energy distribution between PSI and PSII can be fine tuned via LHC state transitions by reversible phosphorylation of certain LHCII proteins (Bonaventura and Myers, 1969; Murata, 1969; Kruse, 2001; Turkina *et al.*, 2006a,b).

Light capture and photoprotection

When solar energy levels exceed energy demand by the cell, LHC transcription is down-regulated to prevent photo-damage (Adir *et al.*, 2003). In contrast, low-light levels lead to increased transcription to maximize photon capture efficiency. Thus, the total amount of LHC proteins and their isoform composition is constantly adjusted to the actual demand for light capture and to changing irradiation conditions.

Besides their role as light energy capture proteins, LHC proteins also fulfil a second role when solar irradiation exceeds photosynthetic capacity. Under these conditions, LHCII proteins facilitate the dissipation of light energy as heat or fluorescence via a mechanism called 'energy-dependent non-photochemical quenching' (NPQ) of chlorophyll fluorescence, which is reported to protect the cell from oxidative damage (Müller *et al.*, 2001). This strategy, however, has the downside that a large proportion of the absorbed photons (~80–95%) are wasted as fluorescence and heat under high-light levels (Polle *et al.*, 2002; Polle *et al.*, 2003), limiting the overall photosynthetic conversion efficiency (Kruse *et al.*, 2005). Despite this, the very existence of these processes indicates that they confer a competitive advantage on the host cell in its natural environment. This is because most plants and photosynthetic microorganisms are limited in mobility and therefore had to develop strategies to adjust to seasonal, diurnal and even daily changes in environmental light levels (e.g. due to varying cloud cover). They have achieved this through the orchestrated interplay of a diverse array of short and long-term adaptation mechanisms (Dietz, 2003).

Light adaptation vs. photon capture efficiency

The cost of having these adaptation mechanisms is reflected in the low light to biomass conversion efficiency of most ecosystems (Prince and Kheshgi, 2005). However for commercial algal bioreactor systems (e.g. for phytochemical and biofuel production) that require high efficiency and in which environmental conditions can be controlled precisely, this ability to adapt to light levels can, at least in theory, largely be dispensed with. With this aim in mind the light-harvesting antenna size can be reduced to minimize efficiency losses and improve light penetration into the bioreactor (Melis *et al.*, 1999; Kruse *et al.*, 2005; Prince and Kheshgi, 2005).

Comparative studies of low (100 μmol/m^2 s) and high (2000 μmol/m^2 s) light adapted *Dunaliella salina* algal cultures (triggering large and smaller light-harvesting complexes, respectively) suggest that cells with reduced

light-harvesting antennae could exhibit two to three times higher photosynthetic capacities in mass culture than normally pigmented cell lines (Neidhardt *et al.*, 1998; Melis *et al.*, 1999). In these experiments, the PSII-LHCII and PSI-LHCI complexes were reported to bind 60 and 100 chlorophylls per reaction centre, respectively. In the absence of the entire antenna system, PSII and PSI are reported to bind ~40 and ~100 chlorophylls per reaction centre (Hankamer *et al.*, 1997; Dekker and Boekema, 2005), respectively. This suggests that the high-light conditions used resulted in the almost complete down-regulation of LHCI and a marked down-regulation of LHCII. However, the limitation of this approach is that it only allows temporary down-regulation.

This paper describes the construction of a *C. reinhardtii* mutant in which the entire LHCI and LHCII antenna complex system has been permanently and almost completely down-regulated and reports its genetic, biochemical, physiological and ultrastructural characterization. These results therefore represent an important step forward in engineering enhanced photon-capture efficiencies in green algal systems.

Results

Screening for LHC mutants

LHCBM1-11 encode the light-harvesting proteins predominantly associated with PSII. These genes are not only highly conserved with respect to one another, but also show homologies to those encoding the LHCI proteins (*LHC1-1-9*) as well as the minor antenna proteins *LHCB4* and *LHCB5*. The most highly conserved region of this gene super family is a region coding for helix 3 of the LHC proteins and shows a region of ~30 bp which is virtually identical in all antenna genes (Supplementary Figure S1). This conserved region was selected as the target for the simultaneous down-regulation of all LHCI and -II proteins using RNAi technology (Fire *et al.*, 1998; Schroda, 2006).

In wild type *C. reinhardtii* some, but not all, LHCII proteins are under the translational control of the cytosolic RNA-binding protein NAB1 (Mussgnug *et al.*, 2005). NAB1 binds and sequesters certain LHCII mRNAs, stabilizing their RNA transcripts and preventing their translation. To avoid any ambiguity caused by the interference of this regulatory pathway with RNAi-induced mRNA degradation, the *NAB1* knockout mutant *Stm3* was chosen as the parental stain.

To generate a LHC-specific RNAi vector, a region of 187 bp with high homology in all LHC genes (see supplementary material Figure S1) was inserted into the vector *MAA7/X-IR* (Rohr *et al.*, 2004) and subsequently transformed into *Stm3*

cells. One hundred and twenty positive transformants were identified through selection on the antibiotic paromomycin (data not shown). These were then screened for effective RNAi through the use of increased concentrations of 5-fluoroindol (5-FL) (Rohr *et al.*, 2004). The *Maa7/X-IR* vector is designed to allow direct and gradual screening for RNAi efficiency by co-silencing the endogenous tryptophan synthase gene together with the target. Tryptophan synthase converts 5-FL in the medium into the toxic tryptophan analogue 5-fluorotryptophan (Rohr *et al.*, 2004). Thus 5-FL-tolerant mutants can be expected to show efficient RNAi for tryptophan synthase and the co-silenced target gene. More than 50% of the 120 transformants survived 30 μM 5-FL which was lethal to the parental strain *Stm3*, suggesting that the construct was expressed to some degree in these transformants. One highly 5-FL-resistant mutant which tolerated up to 90 μM 5-FL in the medium was selected. This strain showed a considerably lighter green phenotype compared to the other colonies (consistent with a mutant in which LHC expression is significantly down-regulated) and was assigned the name *Stm3LR3* (*Stm3 LHC reduction mutant 3*). The fact that *Stm3LR3* survived 5-FL concentrations lethal for parental strain *Stm3* suggests that the light green phenotype was due to the expression of the RNAi construct and not due to a locus-specific gene inactivation caused by random insertion of the RNAi plasmid. However, it has been reported previously that mutations of genes involved in chlorophyll or carotenoid synthesis can result in severe reduction of LHC antenna size (Polle *et al.*, 2001; Polle *et al.*, 2002), which can result in a pale green phenotype (Tanaka *et al.*, 1998). To eliminate the possibility that the light green phenotype of *Stm3LR3* was due to a locus-specific inactivation of a gene (or genes) involved in chlorophyll or carotenoid synthesis, its pigment composition was analysed by thin layer chromatography (Figure 1). The separation of the extracted pigments and their identification by spectroscopy showed that *Stm3LR3* was capable of chlorophyll-a, chlorophyll-b and indeed carotenoid synthesis which are the only pigments known to be bound by the LHC proteins. Thus, taken together with the high resistance to 5-FL, these data indicated that one or more LHC proteins were down-regulated in *Stm3LR3* by RNAi.

Identification of LHCI- and LHCII-specific mRNAs and proteins

To determine whether the LHCI (*LHC1-1* to *LHC1-9*), LHCII (*LHCBM1* to *LHCBM11*) and *LHCB4/LHCB5* mRNA levels were indeed down-regulated, each individual LHC mRNA level was determined by quantitative real-time polymerase chain
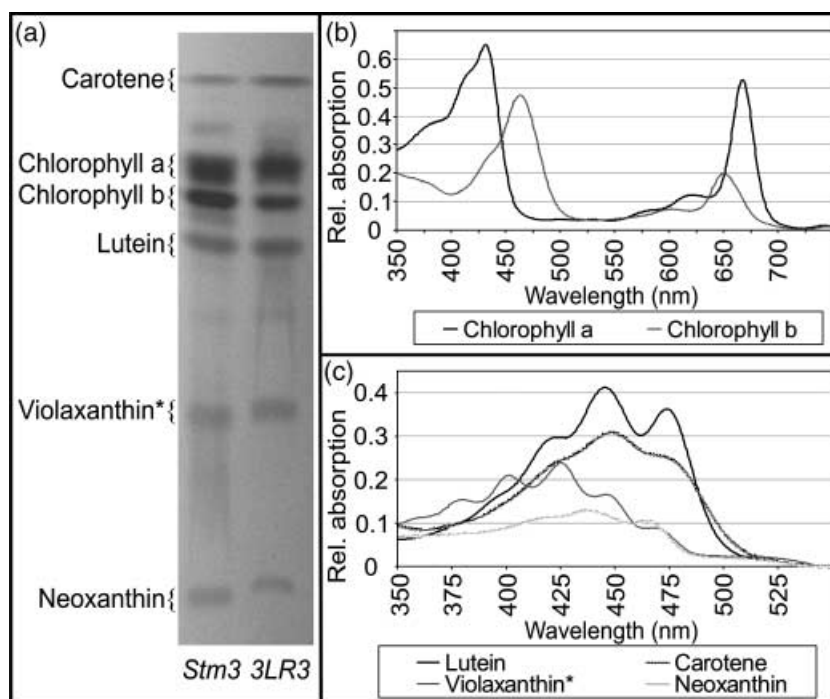
Figure 1 Pigment analysis by thin layer chromatography. Acetone pigment extracts of *Stm3* and *Stm3LR3* (*3LR3*) were applied to a silica gel matrix and separated in petroleum/isopropanol/water (2000 : 220 : 1). Spectra of the individual bands were determined in ethanol. *Indicates a mixture of violaxanthin and violaxanthin derivatives luteoxanthin/auroxanthin as determined by spectroscopy.
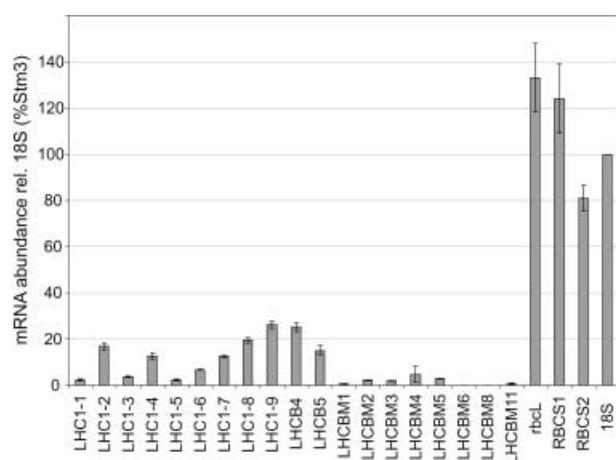

Figure 2 *Stm3LR3* mRNA levels of LHCI genes (*LHC1-1* to *LHC1-9*), *LHCB4*, *LHCB5* and LHCII genes (*LHCBM1-8* and *LHCBM11*) in relation to *Stm3*. Gene expression levels were assessed relative to 18S rRNA abundance (adjusted to 100%) by quantitative real-time PCR. Rubisco genes (*rbcL*, *RBCS1*, *RBCS2*) were used as controls. Error bars = standard error.

reaction (qRT-PCR) using cell cultures in their late logarithmic growth phase (Figure 2). In all cases the LHC mRNA levels in *Stm3LR3* were significantly reduced (subunit specific to 0.1–26%; all *P*-values < 0.016) with respect to the levels observed in the parental strain *Stm3*. The *LHCBM9* mRNA level was already very low and at the limit of detection in *Stm3* (~0.1% of the average *LHCBM* mRNA level), making it impossible to detect further reduction under the experimental conditions. The nuclear encoded genes for ribulose bisphosphate

carboxylase/oxygenase (Rubisco) small subunit (*RBCS1*, *RBCS2*) and the chloroplast encoded gene for Rubisco large subunit (*rbcL*) did not show a significant difference in mRNA abundance. These results clearly indicate that the transformed RNA construct resulted in efficient repression of the expression of all LHC mRNA tested.

To verify LHC reduction at the protein level, denaturing SDS-PAGE and LHC-specific Western analyses were performed with thylakoid membranes of *Stm3* and *Stm3LR3*, with isolated LHC proteins serving as a positive control. The *Stm3* and *Stm3LR3* thylakoid membranes analysed were loaded on an equal chlorophyll basis. Consequently it should be noted that, despite the *Stm3LR3* sample having a higher total protein loading, the LHC bands were still markedly reduced compared to those observed in the *Stm3* lane (Figure 3, Coomassie). This unambiguously shows that LHC proteins levels are greatly reduced in *Stm3LR3*, and this conclusion is supported by the accompanying Western blot (Figure 3, α-LHC) and is in agreement with the qRT-PCR data (Figure 2).

Thylakoid ultrastructure

LHC proteins are reported to play a central role in thylakoid stacking (Barber and Chow, 1979; Allen and Forsberg, 2001; Barber and Nield, 2002; Chow *et al.*, 2005) (Figure 4c). Electron microscopic images (Figure 4a,b) were taken to characterize any morphological changes in thylakoid organization in the mutant *Stm3LR3*.
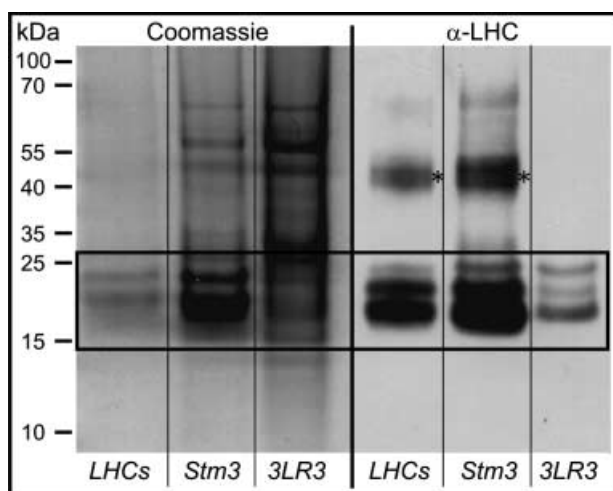
Figure 3 LHC proteins in *Stm3* and *Stm3LR3*. Anti-LHC Western blots with *Stm3* and *Stm3LR3* thylakoid membranes. Left side: Coomassie blue protein stain; right side: anti-LHC Western blot. Samples were loaded on the basis of equal chlorophyll amount (4 µg for the LHC sample, 10 µg for the thylakoid membranes of *Stm3* and *Stm3LR3* (half the amounts for the Western blot). The black box indicates the molecular range of LHC proteins, the asterisks mark higher molecular weight LHC aggregates; the apparent molecular weight is given in kDa.

As reported earlier, *Stm3* shows an increase in thylakoid membrane stacking compared to WT (Mussgnug *et al.*, 2005). In contrast, the images of mutant *Stm3LR3* indicate

that membrane stacking is decreased when LHC antenna proteins are down-regulated. Here, the typical multi-membrane pseudo-granal organization (Figure 4a inset) was replaced by long stretches of parallel double bilayers (Figure 4b inset). To our knowledge, this thylakoid organization has not been described for green algae before, but is very similar to the membrane organization observed in chlorophyll-b-less wheat mutant *CD3* and chlorophyll-b-less barley mutant *chlorina f2* when grown under special light conditions which trigger the down-regulation of all LHC proteins (Allen *et al.*, 1988; Krol *et al.*, 1995).

Our results underline the importance of LHC proteins for membrane organization in *Chlamydomonas*. In contrast to the chlorophyll-b-deficient mutants *CD3* and *chlorina f2*, where special light conditions had to be applied to trigger complete LHC depletion and concomitant unstacking of the thylakoid membranes, *Stm3LR3* did not show stacking under constant, standard illumination of 100 µmol/m^2 s white light, indicating that very low levels of LHC proteins were present. Despite this, the rate of photosynthesis was clearly sufficient to support photosynthetic growth on minimal medium (not shown).

To provide a more detailed phenotypic description, the isolated thylakoid membranes of *Stm3* and *Stm3LR3* were
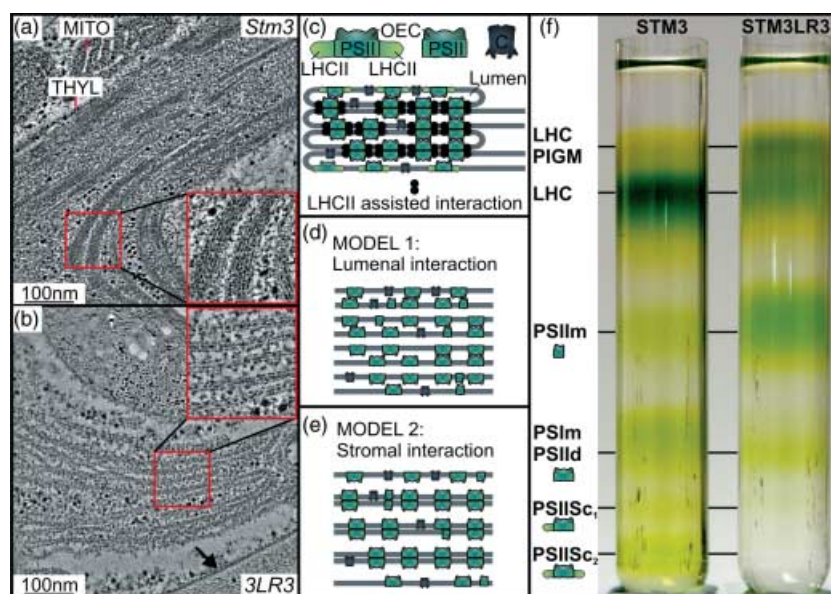

Figure 4 Electron microscopic images, models of membrane interaction and sucrose gradients of *Stm3* and *Stm3LR3* (*3LR3*). (a) *Stm3* section showing extensive granal stacks, consisting of a large number of tightly packed bilayers. (b) *Stm3LR3* section showing the corrrelation between light-harvesting complex (LHC) reduction and the disaggregation of the granal stacks, into bilayer pairs. The red inset boxes show ×2 magnified views of *A* or *B*, respectively. The black arrow in *B* marks a single bilayer. (c) Model of normal thylakoid stacking in the presence of LHC. The black dots indicate the involvement of LHCs in the stacking process. C: cytochrome b6/f complex, OEC: oxygen-evolving complex. (d) Illustrates membrane organization Model 1 in which bilayer pairs are formed via lumenal interactions. (e) Illustrates membrane organization Model 2 in which bilayer pairs are formed via stromal interactions with markedly increased lumenal volume. (f) Sucrose gradient separation of photosynthetic complexes form thylakoid membranes of *Stm3* and *Stm3LR3* (equal chlorophyll loading). Chlorophyll containing bands are indicated. LHC PIGM = LHC pigments and low levels of proteins; LHC = LHC proteins; PSIIm = PSII monomers; PSIm = PSI monomers; PSIId = PSII dimers; PSIISc$_1$ = PSII-LHCII supercomplex1; PSIISc$_2$ = PSII-LHCII supercomplex 2.

gently solubilized with dodecyl maltoside and resolved into their component photosynthetic complexes by sucrose density gradient centrifugation (loaded on an equal chlorophyll basis). The results clearly show that the bottom two bands (PSIISc1 and PSIISc2) are absent in *Stm3LR3* (Figure 4f). The PSIISc2 band is enriched in the classical PSII-LHCII super-complex reported by Boekema *et al.* (1995) and consists of a central PSII core dimer flanked by two LHC antenna sets (the PSIISc1 lacks one of these antenna sets). The fact that *Stm3LR3* lacks the PSIISc1 and PSIISc2 super-complexes is consistent with the down-regulation of the LHC proteins. As the *Stm3* and *Stm3LR3* samples were loaded on an equal chlorophyll (not equal cell) basis, it can be seen that the abundance of LHC:PSIIm (monomer) ratio is much lower in *Stm3LR3* than in *Stm3*, consistent with an overall reduction in LHC proteins.

Chlorophyll parameters, fluorescence properties and light transmission

Optical transmission microscopy (Figure 5a) showed that at the level of the individual cell, the *Stm3LR3* strain had a markedly lower chlorophyll content than the parental *Stm3* control (consistent with the down-regulation of LHC gene expression). This has the effect that when cultures were adjusted to the same cell number (6×10^6 cells/mL), *Stm3LR3*

cultures had a total chlorophyll content of 32% (± 0.95 SE) of that of *Stm3* (Figure 5b). Furthermore, the chlorophyll-a/b ratio in *Stm3LR3* was significantly increased from 1.95 (± 0.12 SE) in *Stm3* to 4.05 (± 0.1 SE), as expected for LHC-deficient strains (Hankamer *et al.*, 1997; Melis *et al.*, 1999; Andersson *et al.*, 2003). The reduced chlorophyll content in *Stm3LR3* led to higher light levels at the centre of 650 mL bioreactors (~290% compared with *Stm3* at optical density $(OD)_{750nm} = 1.0$) when illuminated with 750 µmol/m^2 s white light (not shown).

To measure the effects of the down-regulation of the antenna on fluorescence, *Stm3* and *Stm3LR3* were next analysed using confocal laser scanning microscopy (Figure 5c). Mixtures as opposed to pure samples of the two strains were analysed to ensure their direct comparison under identical imaging conditions. To identify each cell type within the mixed population, *Stm3* or *Stm3LR3* were individually labelled with a green fluorescent marker (MitoTracker® FM) in two separate experiments. Panels I–IV in Figure 5(c) show the results of experiment one, in which *Stm3* was labelled with the green marker. Panels V–VIII in Figure 5(c) show the results of experiment two, in which *Stm3LR3* cells were labelled with the green marker. In both experiments, the mixtures were imaged under four conditions. Panels I and V show the cells imaged in the normal optical mode. Six *Chlamydomonas* cells are seen in panel I; five cells in panel V.
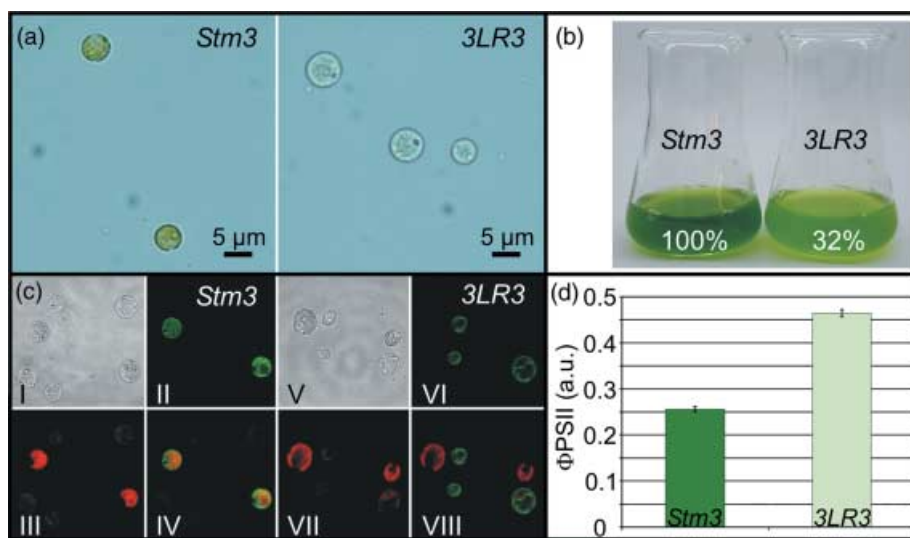

Figure 5 Phenotypic analysis of *Stm3LR3*. (a) Microscopic images of *Stm3* and *Stm3LR3* cells. (b) Cultures of *Stm3* and *Stm3LR3* (*3LR3*) after heterotrophic growth and adjustment to equal cell numbers (6×10^6 cells/mL). Relative chlorophyll concentrations are indicated (*Stm3* set to 100%, ± 0.95 SE). (c) Chlorophyll fluorescence of *Stm3* and *Stm3LR3* cells estimated by confocal laser scanning microscopy in mixed cultures. Panels I–IV: experiment one in which *Stm3* cells were pre-labelled (green). Panels V–VIII: experiment two in which *Stm3LR3* cells were pre-labelled (green). Panels I and V: microscopic image of all cells. Panels II and VI: identification of *Stm3* (panel I) and *Stm3LR3* (panel VI) cells by separate pre-labelling using MitoTracker® FM green fluorescence. Panels III and VII: chlorophyll fluorescence (*red*). Panels IV and VIII: merged images of green and red fluorescence. (d) Photosynthetic quantum yield (φPSII) of *Stm3* and *Stm3LR3*. Fluorescence parameters Ft and F'm were recorded during actinic illumination of liquid cultures and φPSII was calculated according to Maxwell and Johnson (2000), (φPSII = (F'm/Ft)/F'm). a.u. = arbitrary units. Error bars = standard error.

Next the cells were imaged in a fluorescence mode which visualized the green fluorescent marker to identify which cells were *Stm3* and which were *Stm3LR3*. In experiment one, this mode (panel II) shows that two of the six cells were *Stm3* (green). Similarly, in experiment two (panel VI) three of the five cells were identified as *Stm3LR3* (green). To measure chlorophyll fluorescence, the mixed samples were then excited with an actinic light (0.21 mW, 543 nm) before measuring chlorophyll fluorescence (653–718 nm pass filter). In experiments one and two (panels III and VII), only the parental *Stm3* cells fluoresced strongly (red), consistent with their large antenna system. In contrast *Stm3LR3* appeared to have a near 'null fluorescence' phenotype under these conditions.

For control purposes, panels IV and VIII display an overlaid image of the marker-derived fluorescence (green), and the chlorophyll fluorescence (red). These results unambiguously demonstrate that the reduction of the LHC antenna size in *Stm3LR3 has* resulted in a strong down-regulation of fluorescence.

To determine whether the observed reduction of fluorescence translates to improved photon capture efficiencies, maximum quantum yield of PSII (Fv/Fm = (Fm–F0)/Fm) and photosynthetic quantum yield (ϕPSII = F'm–Ft/F'm) (Maxwell and Johnson, 2000) were determined (Figure 5d). Fv/Fm was similar for *Stm3* (0.711, ± 0.016 SE) and *Stm3LR3* (0.767, ± 0.005 SE), indicating efficient PSII primary activity (from water to Q_A) in both strains. To determine the levels of fluorescence losses during illumination, photosynthetic quantum yield was measured. F'm corresponds to the maximal fluorescence while Ft corresponds to the minimal fluorescence during illumination with actinic light (815 μmol/m^2 s white light). In theory, if 100% of the photons captured by the LHCII antenna are used to drive the PSII photochemistry, a ϕPSII value of 1 is expected. In contrast if all the energy is dissipated through the process of fluorescence, ϕPSII would equal 0. Therefore, the parameter ϕPSII can give a good indication of the photon capture efficiency. Under illumination with photosynthetically active radiation at which the parental strain *Stm3* had ϕPSII values of 0.256 (± 0.05 SE), the ϕPSII value of *Stm3LR3* was ~81% higher at 0.464 (± 0.008 SE) (Figure 5d). These results support the confocal microscopy data and suggest that the fluorescence losses of the PSII antenna are significantly lower in the reduced LHC strain.

Reduced photoinhibition and enhanced cell growth at high-light levels

Light induced LHC antenna reduction has previously been reported not only to improve the photosynthetic quantum yield, but to decrease photoinhibition under high-light conditions (Baroli and Melis, 1998). To determine the impact of antenna down-regulation in *Stm3LR3*, photoinhibition trials were conducted using 1400 μmol/m^2 s high light. The level of photoinhibition was determined by measuring the maximal oxygen evolution capacity in 20 min intervals over a period of 100 min. These experiments revealed that under photoinhibitory light conditions, PSII water-splitting activity in *Stm3LR3* maintained a comparable high level of ~40% after 100 min of high-light treatment, compared to only 13% oxygen evolution activity remaining in *Stm3* (Figure 6a). Thus antenna reduction in *Stm3LR3* appears to confer a phenotypic decrease in photoinhibition.

Given the enhanced tolerance of *Stm3LR3* to high-light levels, cultivation experiments were conducted at elevated light conditions of 1000 μmol/m^2 s. These revealed that *Stm3LR3* has not only reduced sensitivity to photoinhibition (Figure 6a) but that cell growth and replication was also significantly faster than that of the parental strain *Stm3* (Figure 6b). Both strains reached similar maximal cell densities
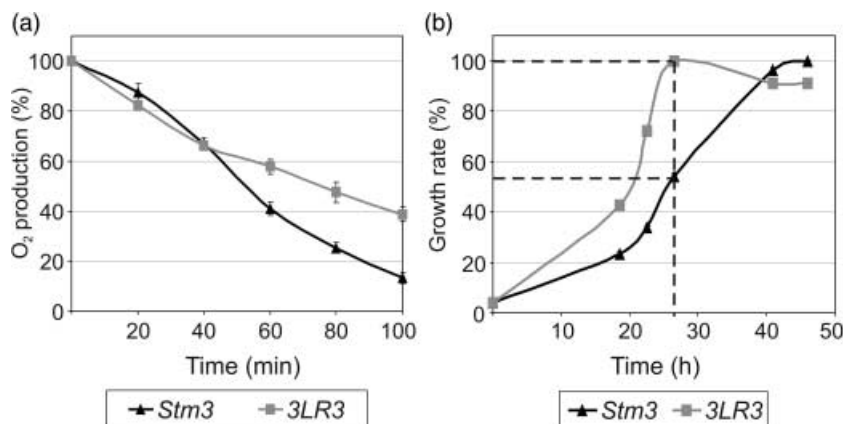

Figure 6 Photoinhibition and growth rates under high-light conditions. (a) O$_2$ production capacity of *Stm3* and *Stm3LR3* (*3LR3*) during photoinhibitory light treatment (1400 μmol/m^2 s for 100 min), determined with a Clark-type oxygen electrode. (b) Mixotrophic growth rates of *Stm3* and *Stm3LR3* (*3LR3*) cultures under continuous high-light conditions (1000 μmol/m^2 s) in TAP medium. Error bars = standard error.

(100% in *Stm3*; 104% in *Stm3LR3*) due to their common ability for mixotrophic growth in tris acetate phosphate (TAP) medium. However, peak density of *Stm3LR3* cultures was detected already after 26.5 h, at which *Stm3* cultures had only been able to grow to 54% of their maximal cell densities (Figure 6b, dotted line).

Discussion

Photosystem and antenna conservation

While photosynthetic core complexes (PSI and PSII) have retained a remarkable degree of conservation between higher plants, green algae and cyanobacteria (Dekker and Boekema, 2005), they have evolved quite different complexes for harvesting solar energy. This reflects their optimal adaptation to specific natural habitats (Grossman *et al.*, 1995). This diversity is presumably linked to the fact that light-harvesting proteins are not only involved in energy capture and transfer, but also fulfil the important role of balancing excitation energy between PSI and PSII (Allen and Forsberg, 2001) and to protect the cells under conditions of excess irradiation (Müller *et al.*, 2001). Furthermore, LHC proteins are thought to be important for maintaining the structural organization of granal thylakoid membrane stacks (Barber and Chow, 1979; Allen and Forsberg, 2001; Chow *et al.*, 2005).

Efficient antenna down-regulation in mutant *Stm3LR3*

Using RNAi technology, the expression of all 20 genes encoding for LHCI, LHCII, CP26 and CP29 were simultaneously and strongly down-regulated in *Stm3LR3* (0.1–26% of *Stm3*; Figures 2–4). This level of permanent LHC reduction has, to our knowledge, not been reported in any algal photosynthetic organism to date.

Pigment synthesis is functional in *Stm3LR3*

The degree of LHC down-regulation appears to be independent of the main biochemical pathways involved in photosynthetic pigment production as chlorophylls a and b, carotene and specifically lutein, violaxanthin and neoxanthin are all produced in *Stm3LR3* (Figure 1). This suggests that the altered thylakoid ultrastructure observed in *Stm3LR3* (Figure 4b) is the direct result of LHC down-regulation and supports previous reports that LHC proteins are involved in membrane stacking (Barber and Chow, 1979; Allen and Forsberg, 2001; Chow *et al.*, 2005).

Thylakoid ultrastructure is altered

Despite major changes in ultrastructure (see bilayer pairs in Figure 4b), *Stm3LR3* is not only capable of photoautotrophic growth but of supporting virtually identical maximal rates of O_2 evolution compared to *Stm3* under saturated light conditions (not shown). This observation indicates that *Stm3LR3* has a fully functional lumen, as in its absence, functional photosynthetic reactions such as the photophosphorylation which are crucial for the cells survival could not be maintained. Currently, two models that fulfil the requirement for an intact lumen, appressed bilayer pairs, and the involvement of LHC proteins in bilayer stacking can be proposed (Figure 4d,e). More experimental data will be required to unambiguously determine which of these two models most accurately describes the *Stm3LR3* phenotype. However, our conclusions are consistent with the observation that *Stm3* (Figure 4a) is enriched in LHCs and exhibits strongly appressed membranes. In *C. reinhardtii* WT strains, which contain less LHC proteins than *Stm3*, less tightly stacked pseudo-grana are observed (Mussgnug *et al.*, 2005).

Chlorophyll fluorescence losses and photoinhibition are decreased in Stm3LR3 while cell growth is enhanced under high-light conditions

The confocal (Figure 5c), φPSII (Figure 5d) and oxygen evolution experiments (Figure 6a) highlight four important properties of *Stm3LR3*. First, LHC down-regulation in this mutant resulted in a decrease in the dissipation of captured light energy through the process of fluorescence (and possibly heat dissipation, although this was not measured). Second, this would be expected to lead to an increase in photosynthetic quantum yield and this was indeed observed (Figure 5d). Third, reducing antenna size reduced the sensitivity of the system to photoinhibition (Figure 6a). Fourth, despite such major antenna reductions the remaining functional photosynthetically active pigments (mainly associated with the PSI and PSII core complexes) were still clearly sufficient to drive photosynthesis efficiently and promoted increased cell growth and replication compared with the parental strain cell cultures (Figure 6b) at elevated light conditions of 1000 µmol/m^2 s.

Biotechnology applications

The *Stm3LR3* phenotype has important implications for biotechnological applications. Photosynthetic microorganisms are increasingly used in large-scale algal culture for the

production of pigments (e.g. β-carotene and astaxanthin), lipids (e.g. polyunsaturated fatty acids) polysaccharides and biomass for biofuel generation (e.g. biodiesel, BTL and bio-H$_2$) (Pulz and Gross, 2004; Rupprecht *et al*., 2006). Compared with higher plants, photosynthetic microorganisms have a number of advantages. Biomass is built up rapidly and production facilities (e.g. open and closed bioreactors) can be sited on non-arable land (eliminating competition with crops required for food production). Closed bioreactors offer the additional advantage that cultures can be maintained under highly controlled conditions (e.g. light, pH, nutrients, temperature) to improve productivity, and in the case of the synthesis of medical products, ensure high quality standards.

The ability to control light conditions in bioreactors is particularly relevant for the work presented here and indeed complements it, as it offers a potential way to increase photosynthetic efficiency levels from ~1–2% (in many ecosystems) towards 10% (Kruse *et al*., 2005). Specifically, regulating the light levels in both open and closed bioreactors by engineering means, reduces the dependence of the organism to regulate excitation energy transfer to the photosynthetic reaction centres and the need for photoprotection strategies via wasteful fluorescence and heat dissipation, which can account for up to ~80–95% of energy loss from the system (Polle *et al*., 2002; 2003), most of which is lost at the illuminated surface of the bioreactor. In this context it should also be noted that for typical wild-type green algae, outdoor condition very rapidly exceeds light utilization capacity during the course of a day [e.g. at mid-latitudes during a cloudless spring day in the Northern Hemisphere, light intensity exceeds light utilization capacity between 7.00 and 17.00 hours (Melis *et al*., 1999)]. The use of small LHC antenna mutants in light-regulated bioreactors is therefore expected to reduce energy losses and has further benefits in terms of increasing the overall photosynthetic efficiency of the algal culture. In particular, reducing fluorescence and heat losses of this magnitude should result in a considerable improvement in light penetration into the bioreactor. Consequently, a much larger proportion of the cells in the culture can be optimally illuminated by the incident solar irradiation, thereby increasing the overall productivity of the bioreactor. This in turn facilitates the reduction of bioreactor sizes and costs that are directly dependent on the efficiency of solar energy conversion (Prince and Kheshgi, 2005). Alternatively, higher cell densities can be used.

In conclusion, RNAi technology has enabled us to downregulate almost the entire LHC antenna system (0.1–26%, subunit specific). Analysis of the thylakoid ultrastructure indicated that this LHC down-regulation reduces interactions between adjacent thylakoid membrane pairs within the granal stacks consistent with the loss of PSII supercomplexes (Figure 4f) which have been postulated to mediate bilayer stacking (Barber and Chow, 1979; Allen and Forsberg, 2001; Barber and Nield, 2002; Chow *et al*., 2005). *Stm3LR3* also showed a number of high light-related phenotypes (reduced fluorescence losses, increased photosynthetic quantum yield, increased resistance to photoinhibition and faster growth rate at elevated light levels) that could have important implications for improved algal cultivation at natural light conditions. In terms of biotechnological applications, the optimization of photosynthetic light capture is central to the enhancement of photosynthetic efficiency for the improved production of photosynthetic biofuels (e.g. bio-ethanol, biodiesel, bio-H$_2$, BTL) and a wide range of other products of large-scale algal culture.

Experimental procedures

Strains and culture conditions

The mutant *Stm3* was generated as described before (Mussgnug *et al*., 2005). Liquid cultures of *C. reinhardtii* were grown in continuous white light (100 µmol/m^2 s). Media for mixotrophic growth (TAP) and photoautotrophic growth (high salt medium) were prepared as described (Harris, 1989). Ten milligram per litre paromomycin (Sigma) and 1.5 mM L-tryptophan (Sigma) were added for screening for *pAlkk1*- and *MAA7/X-IR*-positive transformants. Plates with 30–90 µM 5-fluoroindole (Sigma) were prepared to re-screen transformants for efficient RNAi.

RNAi vector construction and transformation

Manipulations of nucleic acids were performed following standard methods (Sambrook *et al*., 1989). A 187-bp region (separated by a spacer of 145 bp) was selected for RNAi to suppress gene expression of all LHC gene isoforms. The selected sequence (corresponding to nucleotides 527–713 3′ from the cDNA start codon) was amplified by PCR using *LHCBM1* cDNA as template (sense primers: cg*gaattc*gcctggacaagctgtaccc-gc*tctaga*aggtggtcggacaggttc, antisense primers: cg*gaattc*gcctggacaagctgtaccc-gc*tctaga*accagaccacac-aagacgac, *Xba*I and *Eco*RI restriction sites are in italics) cloned in sense–antisense orientation via the *Xba*I site and inserted into RNAi vector *MAA7/X-IR* (Rohr *et al*., 2004) via the *Eco*RI site. This LHC-RNAi vector (*pAlkk1*) was then transformed into *C. reinhardtii* strain *Stm3* by glass bead transformation (Kindle, 1990).

RNA isolation and cDNA synthesis

Four biological replicates of total RNA were isolated from 10 mL of *C. reinhardtii culture* (OD$_{750nm}$ = 1.0) using Promega™ SV RNA Isolation Kit. First strand cDNA was synthesized using 2 µg total RNA and the Superscript III™ RT (Invitrogen) protocol with the

following amendments: enzyme 0.5 μL, oligo-dT (0.2 μL of 100 μM) and random hexamer (0.05 μL of 3 μg/μL) primers. Following synthesis, cDNA was diluted to 5 ng/μL.

Quantitative real-time PCR (qRT-PCR)

qRT-analysis was carried out in ABI optical 384-well plates using an ABI PRISM© 7900 HT Sequence Detection System (Applied Biosystems) and the standard thermal profile and dissociation stage. Each reaction contained 3 μL SYBR® Green 2× Master Mix, 5 ng of cDNA, and 200 nM of each gene-specific primer pair to a final volume of 6 μL. PCR reagents were aliquoted into 384-well plates using an Eppendorf Epmotion 5075™ Liquid Handler. The PCR primer efficiency (*E*-value) was calculated as previously described (McGrath *et al.*, 2005). Gene expression levels relative to 18S rRNA were calculated for each cDNA sample using the equation: relative ratiogene/18S rRNA = (Egene (–Ct gene))/(E18S rRNA(–Ct 18S rRNA)). The average ratios of the four *Stm3* and four *Stm3LR3* samples were used to determine the fold-change in transcript level between *Stm3* and *Stm3LR3*. For the primers used see supplementary material Table S1.

Chlorophyll fluorescence measurements

For fluorescence microscopy, 500 μL of *Stm3* and *Stm3LR3* cultures was harvested by centrifugation and re-suspended in 300 μL TAP. A total of 0.1 μL MitoTracker® Green FM (Molecular Probes, 35 nM final concentration) was added, and cell suspensions were incubated for 45 min in the dark. Cells were collected by centrifugation, washed twice and re-suspended in 100 μL TAP. Mixtures (1 : 1) of labelled *Stm3* with unlabelled *Stm3LR3* cell suspensions, or the converse, unlabelled *Stm3* with labelled *Stm3LR3* cells were prepared and fluorescence signals were recorded (Zeiss LSM 510 META). All chlorophyll fluorescence parameters were determined at room temperature (Mini-PAM, Walz). Fv/Fm was determined after dark incubation of cell suspension (15 μg Chl/mL) for 5 min by recording of F0 and Fm (the latter after application of a saturating light pulse of 15 000 μmol/m^2 s) and calculation of Fv/Fm = (Fm–F0)/Fm (Maxwell and Johnson, 2000). Saturation efficiency of the light pulse was confirmed by addition of 50 μM DCMU and recording of maximal fluorescence levels. Photosynthetic quantum yield (φPSII) was determined by illuminating cell suspensions (15 μg Chl/mL) with actinic white light (815 μmol/m^2 s, saturation pulse of 15 000 μmol/m^2 s). Fluorescence parameters were recorded and quantum yield calculated [φPSII = (F'm–Ft)/F'm (Maxwell and Johnson, 2000)].

Determination of cell growth, chlorophyll content and light transmission

One hundred-millilitre volumes of TAP medium were inoculated with *Stm3* or *Stm3LR3* to OD$_{750nm}$ = 0.03 and growth rates were determined by monitoring OD$_{750nm}$. TAP medium, which includes a fixed carbon source (acetate), to increase the rate of cell growth and reduce cultivation difficulties (e.g. bubbling the cultures with CO$_2$) was used in these experiments. However, the use of minimal medium might be considered in large-scale production facilities to further reduce production costs. The correlation between OD$_{750nm}$ and cell numbers was controlled by counting of the cells in control

samples. Chlorophyll contents (μg/mL) as well as a/b ratios were determined spectroscopically after extraction with 80% acetone (Arnon, 1949). Cultures were illuminated with continuous white light of 1000 μmol/m^2 s to determine growth under elevated light conditions. Light transmission was measured with a spherical light-meter (QSL-2101, Biospherical Instruments Inc.) in the centre of a 650 mL glass reactor after adjusting cell cultures to OD$_{750nm}$ = 1.0.

Photoinhibition measurements

Cell cultures were grown for 2 days, adjusted to OD$_{750nm}$ = 0.2 in TAP medium and then illuminated with 1400 μmol/m^2 s white light for 100 min. Samples were taken in 20 min intervals, 10 mM NaHCO$_3$ added and apparent O$_2$ production measured in a Clark-type oxygen electrode (1400 μmol/m^2 s actinic white light). Respiration was determined at the end of the measurements by dark incubation and subtracted from the apparent O$_2$ production levels.

SDS gel electrophoresis, thin layer chromatography (TLC) and thylakoid membrane preparation

Proteins were separated by SDS gel electrophoresis (Laemmli, 1970) and subsequently electroblotted onto nitrocellulose membranes (Amersham). LHC-specific antibodies, raised against higher plant LHC proteins, were kindly provided by S. Jansson and used in conjunction with Anti-Rabbit IgG-AP conjugate (Sigma).

Pigments were separated by TLC. One hundred and fifty-millilitre liquid cultures of *Stm3* and *Stm3LR3* were grown and harvested as described. Ten-milligram CaCO$_3$ and 5 mL acetone were added to each pellet. The acetone extract was then filtered and applied on silica TLC plates (10 × 20 cm, Sigma). A petroleum/isopropanol/water (2000 : 220 : 1) mixture was used as the running solvent for pigment separation. Absorption spectra were taken to confirm pigment identity by resuspending separated pigments in ethanol, centrifuging (5 min 18 000 *g*) and scanning the absorption spectra of the supernatant (range 350 nm to 750 nm, Varian Cary 50 UV/VIS Bio-Spectrophotometer).

For thylakoid membrane purification, 300 mL of *Stm3* and *Stm3LR3* cells was grown to late log phase, adjusted to equal OD$_{750nm}$ values, centrifuged (10 min, 2200 *g*, 4 °C) and washed by re-suspending in 30 mL of buffer A (25 mM HEPES pH 7.5, 1 mM MgCl$_2$, 0.3 M sucrose). The washed cells were then pelleted by centrifugation (10 min, 2200 *g*, 4 °C), before being re-suspended in 8 mL of buffer A and sheared open by two two passes through a French Press (2000 psi, 4 °C). The sample volume was then increased to 30 mL (buffer A) and the thylakoid membranes were precipitated through centrifugation (45 min, 20 000 *g*, 4 °C). To wash the thylakoid membranes they were re-suspended in 30 mL buffer B (5 mM HEPES, pH 7.5, 10 mM EDTA, 0.3 M sucrose) and pelleted (45 min, 4 °C, 48 000 *g*). The thylakoid membranes were then re-suspended in 2.65 mL of buffer B and 1 mL buffer C (5 mM HEPES, pH 7.5, 10 mM EDTA, 2.2 M sucrose), to adjust the final sucrose concentration (not including volume of the pellet) to 1.82 mM. This suspension was then dispensed into a Beckman SW32Ti centrifugation tube, before being overlaid with 1.75 M sucrose solution [half the volume of tube (15.3 mL)], and a further layer (5 mL) of buffer D (5 mM HEPES, pH 7.5, 0.5 M sucrose) before centrifuging (60 min, 100 000 *g*, 4 °C). The centrifuged thylakoid membrane sample formed a dense

green band at the position of the sucrose cushion step. Upon harvesting, the sample was diluted with 5 volumes of buffer E (20 mM MES, pH 6.3, 5 mM MgCl$_2$, 15 mM NaCl, 10% (v/v) glycerol) to facilitate pelleting of the purified thylakoid membranes on centrifugation (20 min, 40 000 g, 4 °C). The thylakoid membranes were then re-suspended in a minimal volume (~1 mL) of MMNB buffer (25 mM MES, pH 6.0, 5 mM MgCl$_2$, 10 mM NaCl, 2 M Betaine) and flash frozen in liquid N$_2$ prior to storage at −80 °C. LHC proteins were isolated from the thylakoid membranes by solubilizing the samples in 33 mM β-dodecyl maltoside (500 μL final volume) and resolving them on a sucrose density gradient (16 h, ~250 000 g, 4 °C). Sucrose gradients were formed by freeze-thawing centrifuge tubes filled with 25 mM Mes pH 5.5, 500 mM sucrose, 10 mM NaCl, 5 mM CaCl$_2$, 10 mM NaHCO$_3$, and 0.03% β-dodecyl maltoside according to Hankamer *et al*. (1997).

Electron microscopy of cell sections

For transmission electron microscopy, cells were grown in TAP medium to an OD$_{750nm}$ of 1.0 in continuous white light (100 μmol/m^2 s). Samples were pelleted gently at 1000 r.p.m. in 15 mL of culture medium. An equal volume of 20% bovine serum albumin and 20% dextran in phosphate-buffered saline (PBS) was then mixed with the cell pellet. Aliquots of cells, concentrated by centrifugation in heat-sealed micropipette tips, were then applied to 200 micron Leica wells and high-pressure frozen using a Leica Empact 2 system. Frozen cells were freeze substituted in 2% OsO$_4$ for a week using the Leica AFS system. Samples were rinsed with dry fresh acetone at the end of freeze substitution and embedded in epon resin. Resin blocks were sectioned at 80 nm thickness (Leica Ultramicrotome UC6), and sections were stained with uranyl acetate/lead citrate and imaged at 300 keV (FEI F30 electron microscope, equipped with a GATAN 4 × 4K CCD camera).

Acknowledgements

References

Adir, N., Zer, H., Shochat, S. and Ohad, I. (2003) Photoinhibition – a historical perspective. *Photosynth. Res*. **76**, 343–370.

Allen, K.D., Duysen, M.E. and Staehelin, L.A. (1988) Biogenesis of thylakoid membranes is controlled by light intensity in the conditional chlorophyll b-deficient CD3 mutant of wheat. *J. Cell Biol*. **107**, 907–919.

Allen, J.F. and Forsberg, J. (2001) Molecular recognition in thylakoid structure and function. *Trends Plant Sci*. **6**, 317–326.

Andersson, J., Wentworth, M., Walters, R.G., Howard, C.A., Ruban, A.V., Horton, P. and Jansson, S. (2003) Absence of the Lhcb1 and Lhcb2 proteins of the light-harvesting complex of photosystem II – effects on photosynthesis, grana stacking and fitness. *Plant J*. **35**, 350–361.

Arnon, D.I. (1949) Copper enzymes in isolated chloroplasts – polyphenoloxidase in beta vulgaris. *Plant Physiol*. **24**, 1–15.

Barber, J. and Chow, W.S. (1979) Mechanism for controlling the stacking and unstacking of chloroplast thylakoid membranes. *FEBS Lett*. **105**, 5–10.

Barber, J. and Nield, J. (2002) Organization of transmembrane helices in photosystem II: comparison of plants and cyanobacteria. *Phil. Trans. R. Soc. B Biol. Sci*. **357**, 1329–1335.

Baroli, I. and Melis, A. (1998) Photoinhibitory damage is modulated by the rate of photosynthesis and by the photosystem II light-harvesting chlorophyll antenna size. *Planta*, **205**, 288–296.

Boekema, E.J., Hankamer, B., Bald, D., Kruip, J., Nield, J., Boonstra, A.F., Barber, J. and Rogner, M. (1995) Supramolecular structure of the photosystem II complex from green plants and cyanobacteria. *Proc. Natl. Acad. Sci. USA*, **92**, 175–179.

Bonaventura, C. and Myers, J. (1969) Fluorescence and oxygen evolution from *Chlorella pyrenoidosa*. *Biochim. Biophys. Acta*, **189**, 366–386.

Chow, W.S., Kim, E.H., Horton, P. and Anderson, J.M. (2005) Granal stacking of thylakoid membranes in higher plant chloroplasts: the physicochemical forces at work and the functional consequences that ensue. *Photochem. Photobiol. Sci*. **4**, 1081–1090.

Dekker, J.P. and Boekema, E.J. (2005) Supramolecular organization of thylakoid membrane proteins in green plants. *Biochim. Biophys. Acta-Bioenergetics*, **1706**, 12–39.

Dietz, K.J. (2003) Redox control, redox signaling, and redox homeostasis in plant cells. *Int. Rev. Cytol*. **228**, 141–193.

Durnford, D.G., Price, J.A., McKim, S.M. and Sarchfield, M.L. (2003) Light-harvesting complex gene expression is controlled by both transcriptional and post-transcriptional mechanisms during photoacclimation in *Chlamydomonas reinhardtii*. *Physiol. Plantarum*, **118**, 193–205.

Elrad, D. and Grossman, A.R. (2004) A genome's-eye view of the light-harvesting polypeptides of *Chlamydomonas reinhardtii*. *Curr. Genet*. **45**, 61–75.

Escoubas, J.M., Lomas, M., Laroche, J. and Falkowski, P.G. (1995) Light intensity regulation of Cab gene transcription is signaled by the redox state of the plastoquinone pool. *Proc. Natl. Acad. Sci. USA*, **92**, 10 237–10 241.

Fire, A., Xu, S.Q., Montgomery, M.K., Kostas, S.A., Driver, S.E. and Mello, C.C. (1998) Potent and specific genetic interference by double-stranded RNA *in Caenorhabditis elegans*. *Nature*, **391**, 806–811.

Flachmann, R. and Kühlbrandt, W. (1995) Accumulation of plant antenna complexes is regulated by posttranscriptional mechanisms in tobacco. *Plant Cell*, **7**, 149–160.

Grossman, A.R., Bhaya, D., Apt, K.E. and Kehoe, D.M. (1995) Light-harvesting complexes in oxygenic photosynthesis: Diversity, control, and evolution. *Annu. Rev. Genet*. **29**, 231–288.

Hankamer, B., Nield, J., Zheleva, D., Boekema, E., Jansson, S. and Barber, J. (1997) Isolation and biochemical characterisation of monomeric and dimeric photosystem II complexes from spinach and their relevance to the organisation of photosystem II in vivo. *Eur. J. Biochem*. **243**, 422–429.

Harris, E.H. (1989) *The* Chlamydomonas *Sourcebook: A Comprehensive Guide to Biology and Laboratory Use*. San Diego, CA: Academic Press.

Jansson, S. (1999) A guide to the Lhc genes and their relatives in Arabidopsis. *Trends Plant Sci.* **4**, 236–240.

Kindle, K.L. (1990) High-frequency nuclear transformation of *Chlamydomonas reinhardtii. Proc. Natl. Acad. Sci. USA*, **87**, 1228–1232.

Krol, M., Spangfort, M.D., Huner, N.P.A., Oquist, G., Gustafsson, P. and Jansson, S. (1995) Chlorophyll a/b binding proteins, pigment conversions, and early light-induced proteins in a chlorophyll b-less barley mutant. *Plant Physiol.* **107**, 873–883.

Kruse, O. (2001) Light-induced short-term adaptation mechanisms under redox control in the PSII-LHCII supercomplex: LHC II state transitions and PSII repair cycle. *Naturwissenschaften*, **88**, 284–292.

Kruse, O., Rupprecht, J., Mussgnug, J.H., Dismukes, G.C. and Hankamer, B. (2005) Photosynthesis: a blueprint for solar energy capture and biohydrogen production technologies. *Photoch. Photobio. Sci.* **4**, 957–970.

Laemmli, U.K. (1970) Cleavage of structural proteins during assembly of the head of bacteriophage T4. *Nature*, 227, 680–685.

Legen, J., Misera, S., Herrmann, R.G. and Meurer, J. (2001) Map positions of 69 *Arabidopsis thaliana* genes of all known nuclear encoded constituent polypeptides and various regulatory factors of the photosynthetic membrane: a case study. *DNA Res.* **8**, 53–60.

Lindahl, M., Yang, D.H. and Andersson, B. (1995) Regulatory proteolysis of the major light-harvesting chlorophyll a/b protein of photosystem II by a light-induced membrane-associated enzymatic system. *Eur. J. Biochem.* **231**, 503–509.

Maxwell, K. and Johnson, G.N. (2000) Chlorophyll fluorescence – a practical guide. *J. Exp. Bot.* **51**, 659–668.

McGrath, K.C., Dombrecht, B., Manners, J.M., Schenk, P.M., Edgar, C.I., Maclean, D.J., Scheible, W.R., Udvardi, M.K. and Kazan, K. (2005) Repressor- and activator-type ethylene response factors functioning in jasmonate signaling and disease resistance identified via a genome-wide screen of *Arabidopsis* transcription factor gene expression. *Plant Physiol.* **139**, 949–959.

Melis, A., Neidhardt, J. and Benemann, J.R. (1999) *Dunaliella salina* (Chlorophyta) with small chlorophyll antenna sizes exhibit higher photosynthetic productivities and photon use efficiencies than normally pigmented cells. *J. Appl. Phycol.* **10**, 515–525.

Müller, P., Li, X.P. and Niyogi, K.K. (2001) Non-photochemical quenching. A response to excess light energy. *Plant Physiol.* **125**, 1558–1566.

Murata, N. (1969) Control of excitation transfer in photosynthesis. Light-induced change of chlorophyll a fluorescence in *Porphyridium cruentum. Biochim. Biophys. Acta*, **172**, 242–251.

Mussgnug, J.H., Wobbe, L., Elles, I., Claus, C., Hamilton, M., Fink, A., Kahmann, U., Kapazoglou, A., Mullineaux, C.W., Hippler, M., Nickelsen, J., Nixon, P.J. and Kruse, O. (2005) NAB1 is an RNA binding protein involved in the light regulated differential expression of the light harvesting antenna of *Chlamydomonas reinhardtii. Plant Cell*, **17**, 3409–3421.

Neidhardt, J., Benemann, J.R., Zhang, L.P. and Melis, A. (1998) Photosystem-II repair and chloroplast recovery from irradiance stress: relationship between chronic photoinhibition, light-harvesting chlorophyll antenna size and photosynthetic productivity in *Dunaliella salina* (green algae). *Photosynth. Res.* **56**, 175–184.

Polle, J.E.W., Kanakagiri, S., Jin, E., Masuda, T. and Melis, A. (2002) Truncated chlorophyll antenna size of the photosystems – a practical method to improve microalgal productivity and hydrogen production in mass culture. *Int. J. Hydrogen Energ*, **27**, 1257–1264.

Polle, J.E.W., Kanakagiri, S.D. and Melis, A. (2003) tla1, a DNA insertional transformant of the green alga *Chlamydomonas reinhardtii* with a truncated light-harvesting chlorophyll antenna size. *Planta*, **217**, 49–59.

Polle, J.E.W., Niyogi, K.K. and Melis, A. (2001) Absence of lutein, violaxanthin and neoxanthin affects the functional chlorophyll antenna size of photosystem II but not that of photosystem I in the green alga *Chlamydomonas reinhardtii. Plant Cell Physiol.* **42**, 482–491.

Prince, R.C. and Kheshgi, H.S. (2005) The photobiological production of hydrogen: potential efficiency and effectiveness as a renewable fuel. *Crit. Rev. Microbiol.* **31**, 19–31.

Pulz, O. and Gross, W. (2004) Valuable products from biotechnology of microalgae. *Appl. Microbiol. Biot.* **65**, 635–648.

Rohr, J., Sarkar, N., Balenger, S., Jeong, B.R. and Cerutti, H. (2004) Tandem inverted repeat system for selection of effective transgenic RNAi strains in *Chlamydomonas. Plant J.* **40**, 611–621.

Rupprecht, J., Hankamer, B., Mussgnug, J.H., Ananyev, G., Dismukes, C. and Kruse, O. (2006) Perspectives and advances of biological H-2 production in microorganisms. *Appl. Microbiol. Biot*, **72**, 442–449.

Sambrook, J., Fritsch, E.F. and Maniatis, T. (1989) *Molecular Cloning: a Laboratory Manual*. Cold Spring Harbor, NY: Cold Spring Harbor Laboratory Press.

Schroda, M. (2006) RNA silencing in *Chlamydomonas*: mechanisms and tools. *Curr. Genet.* **49**, 69–84.

Takahashi, Y., Yasui, T., Stauber, E.J. and Hippler, M. (2004) Comparison of the subunit compositions of the PSI-LHCI supercomplex and the LHCI in the green alga *Chlamydomonas reinhardtii. Biochemistry*, **43**, 7816–7823.

Tanaka, A., Ito, H., Tanaka, R., Tanaka, N.K., Yoshida, K. and Okada, K. (1998) Chlorophyll a oxygenase (CAO) is involved in chlorophyll b formation from chlorophyll a. *Proc. Natl. Acad. Sci. USA*, **95**, 12 719–12 723.

Tokutsu, R., Teramoto, H., Takahashi, Y., Ono, T.A. and Minagawa, J. (2004) The light-harvesting complex of photosystem I in *Chlamydomonas reinhardtii*: Protein composition, gene structures and phylogenic implications. *Plant Cell Physiol.* **45**, 138–145.

Turkina, M.V., Blanco-Rivero, A., Vainonen, J.P., Vener, A.V. and Villarejo, A. (2006a) CO_2 limitation induces specific redox-dependent protein phosphorylation in *Chlamydomonas reinhardtii. Proteomics*, **6**, 2693–2704.

Turkina, M.V., Kargul, J., Blanco-Rivero, A., Villarejo, A., Barber, J. and Vener, A.V. (2006b) Environmentally modulated phosphoproteome of photosynthetic membranes in the green alga *Chlamydomonas reinhardtii. Mol. Cell Proteomics*, **5**, 1412–1425.

Zwart, R.W.R., Boerrigter, H. and van der Drift, A. (2006) The impact of biomass pretreatment on the feasibility of overseas biomass conversion to Fischer-Tropsch products. *Energ. Fuel*, **20**, 2192–2197.

Supplementary Material

The following supplementary material is available for this article:

Figure S1 Alignment (CLUSTAL W) of all LHC genes and of the region selected for RNAi. Black: 100% sequences identity, grey shades: sequence homology.

Table S1 List of qRT primers (5′–3′orientation).

This material is available as part of the online article from:
http://www.blackwell-synergy.com/doi/abs/10.1111/
j.1467-7652.2007.00285.x
(This link will take you to the article abstract).

Please note: Blackwell Publishing is not responsible for the content or functionality of any supplementary materials supplied by the authors. Any queries (other than missing material) should be directed to the corresponding author for the article.